

# Analytical Modelling Segmented Switched Reluctance Linear Synchronous Motor (SSRLSM) Using Permeance Analysis Model (PAM)

Norrimah Abdullah<sup>1,2,3</sup>, Fairul Azhar Abdul Shukor<sup>1,2\*</sup>, Raja Nor Firdaus Kashfi Raja Othman<sup>1,2</sup>, Suhairi Rizuan<sup>4</sup> and Nur Ashikin Mohd Nasir<sup>1,2</sup>

<sup>1</sup>Faculty of Electrical Engineering, Universiti Teknikal Malaysia Melaka (UTeM), 76100 Melaka, Malaysia

<sup>2</sup>Electrical Machine Design, Power Electronics and Drives Research Group, CeRIA, UTeM, 76100 Melaka, Malaysia

<sup>3</sup>Universiti Kuala Lumpur – Malaysia France Institute, 43650, Bandar Baru Bangi, Selangor, Malaysia

<sup>4</sup>Electrical Section, Universiti Kuala Lumpur – Malaysia British Institute, 53100 Gombak, Selangor, Malaysia

\*Corresponding author: fairul.azhar@utem.edu.my

*Submitted 21 December 2023, Revised 13 March 2024, Accepted 16 March 2024, Available online 16 April 2024.*

Copyright © 2024 The Authors.

**Abstract:** This paper discusses the analytical modelling of a segmented switched reluctance linear synchronous motor (SSRLSM) using a magnetic equivalent circuit (MEC) based on the permeance analysis method (PAM). The PAM is applied to obtain the MEC of the SSRLSM, considering the flux path pattern in the air gap region between the stator and mover. The PAM is used to create the air gap permeance model. The developed permeance model was transformed into a MEC. The MEC corresponds to an electrical circuit based on the geometry of the machine and the estimated magnetic flux path to solve the SSRLSM thrust performance analysis. The equation is derived from the MEC of the SSRLSM and used to analyse the characteristics of the thrust performance of the SSRLSM. The effect of mover position and phase current on the thrust is investigated and analysed. To validate the model of the SSRLSM, the thrust characteristics were compared with FEM and measurement results. The comparison shows good agreement.

**Keywords:** Analytical modelling; Linear switched reluctance motor; Magnetic equivalent circuit; Permeance model.

## 1. INTRODUCTION

Switched reluctance linear synchronous motors (SRLSM) are favored for industrial applications due to robust structure, high reliability, and superior thrust performance compared to other electric linear motors [1]–[5]. However, the conventional SRLSM (CSRLSM) suffers from higher thrust ripple, leading to vibration and noise [2][6]. To enhance SRLSM efficiency, particularly torque ripple and thrust performance, researchers have explored novel SRLSM topologies, including segmented stator/rotor SRLMs, dual stator/rotor SRLMs, and axial flux SRLMs [2], [7]–[9]. Among these, the segmented structure SRLSM (SSRLSM) stands out as an excellent solution to reduce thrust ripple and improve overall performance compared to the conventional SRLSM [8], [10]–[12]. Consequently, SSRLSM was chosen for analytical modeling in this study.

The numerical and analytical methods are two techniques for modelling and analysing the electromagnetic (EM) of the motor [13], [14]. These methods serve various optimization objectives, such as minimizing torque ripple, maximizing efficiency, and reducing motor weight.[15]. Finite Element Analysis (FEA) is the best numerical approach to accurately determines the static and dynamic characteristics of SRLSM [1] [4]. However, it is complex and time-consuming due to the need for volume meshing across the entire solution domain [5], [16]. In contrast, analytical modelling techniques allow early-phase analysis of thousands of candidate motors. It eliminate infeasible machine solutions early in the design process, leading to a smaller set of feasible solutions that can be further optimised, thus significantly reducing computation time and ensuring sufficient accuracy FEA [10] [11].

Magnetic equivalent circuit (MEC) is a fast and excellent analytical modelling technique and provides reasonably accurate solutions with less computational effort [12], [13], [15], [17]–[21]. Furthermore, MECs offer a deeper understanding of motor behavior and facilitate easier interpretation and analysis of results [14]. It can accurately account for the air-gap region and consider effects like slots, magneto-motive force drops, and sources [15]. In addition, MECs handle nonlinear factors such as magnetic leakage, fringing flux, and saturation, enhancing the modeling accuracy of SRLSMs [6], [7], [19], [20].

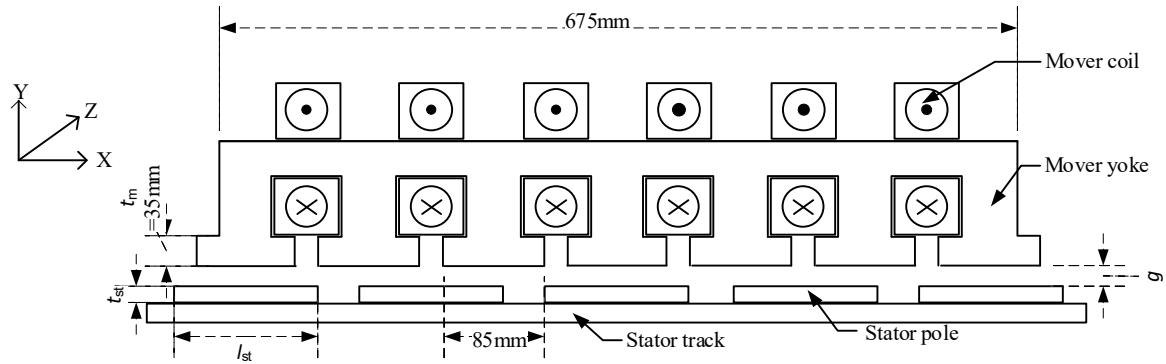


Figure 1. Outline structure of SSRLSM (unit: mm). [22]

This study focuses on analytical modeling for SSRLSMs using MEC. The SSRLSM are emphasized due to its ability to generate more force than conventional SRLSMs [3] [8] [13]. The MEC for SSRLSMs is developed based on the Permeance Analysis Model (PAM). This PAM calculates the permeance of different areas within the motor, that accurately considers the air gap region, slots, magnetic force drops, and sources, thus representing how smoothly magnetic flux flows along specific paths [5] [11]. Each element in the circuit corresponds to a magnetic path and its associated reluctance and can be connected in parallel or series, representing specific parts of the machine geometry [9]. The accuracy of PAM results depends on how closely the magnetic flux estimate matches the actual state. Advantages of the permeance analysis model include determining critical geometry parameters for motor performance, aiding in iterative motor design, and providing insights into static and dynamic motor characteristics [10], [11], [14].

## 2. BASIC PRINCIPLE OF THE SSRLSM

Figure 1 illustrates the basic structure of the 3-phase 6-slot 4-pole SSRLSM. The SSRLSM is designed with a flat structure. This motor has the same structure as the rotary SRM with a segmental stator, described elaborately in [18][22]. The basic structure of SSRLSM has two parts: mover and stator. The mover is comprised of a yoke and coil, while the stator side encompasses a stator track and a segmented stator pole. Both the mover yoke and stator pole are constructed from SS400 material, while the stator track is fabricated using aluminium.

To study the SSRLSM thrust characteristic, the derived formulated expression is considered for thrust determination using PAM i.e., (1) the permeability of the yoke is regarded as infinity and (2) the leakage flux is disregarded. The yoke of the SSRLSM is made of the SS400 material and as it has 300 times more permeability than the air permeability, the value of magnetic resistance inside the yoke is 300 times lower compared to the air. Most of the flux produced by the SSRLSM will flow inside the yoke. Consequently, the calculation result is about 0.3% if this factor is considered. Thus, the air gap permeance is considered in the developed permeance model by referring to the pattern of flux path distributed between the mover and stator obtained from the FEA simulation.

## 3. ANALYTICAL MODELLING OF THE SSRLSM

This study focuses on the development of an analytical model for the SSRLSM. The process is illustrated in Figure 2. Before creating the analytical model, the specific dimensions of a proposed SSRLSM with the highest thrust were determined by optimisation using Finite Element Method (FEM) simulation [22]. The confirmed structure was simulated using FEM to obtain the flux pattern between the mover and the stator, which is used to develop the permeance model. The developed permeance model was then converted to MEC. Finally, the total permeance was calculated for each developed MEC.

Considering the flux path pattern in Figure 3 is the initial step in the analytical modeling of the SSRLSM after the optimisation process. The flux path pattern of the SSRLSM was obtained from simulation using FEM. The magnetic flux path pattern changes with the mover position and phase current. The magnetic flux path is separated into several junctions as a parallel junction, and each intersection will combine back together as a series junction. Each intersection will represent one permeance. In the observation, when the mover moves to the left from 0 mm to 157 mm, for every 3 mm step displacement, the pattern of flux path was recorded. As a sample for the development of analytical modelling of SSRLSM, the pattern of flux path at two critical positions of the mover, at fully aligned and partially aligned positions, were considered and thus the permeance model was developed.

Aligned and partially aligned positions in SSRLSM refer to the position of the mover with respect to the stator. For a fully aligned position, the mover is positioned such that it faces the stator poles with minimal gap. When the coils on the mover are energised in this position, strong magnetic circuit formed, and the magnetic circuit is completed with lower reluctance, and the motor produces maximum force. While, partially aligned, the mover and stator are an intermediate state between fully aligned and fully unaligned, thus some stator poles align with the mover, while others remain offset. As a result, the motor produces a moderate amount of force when the coils are energised, less than the aligned position but more than the unaligned position. This position represents any state of the translator during its movement that is not fully aligned or unaligned.

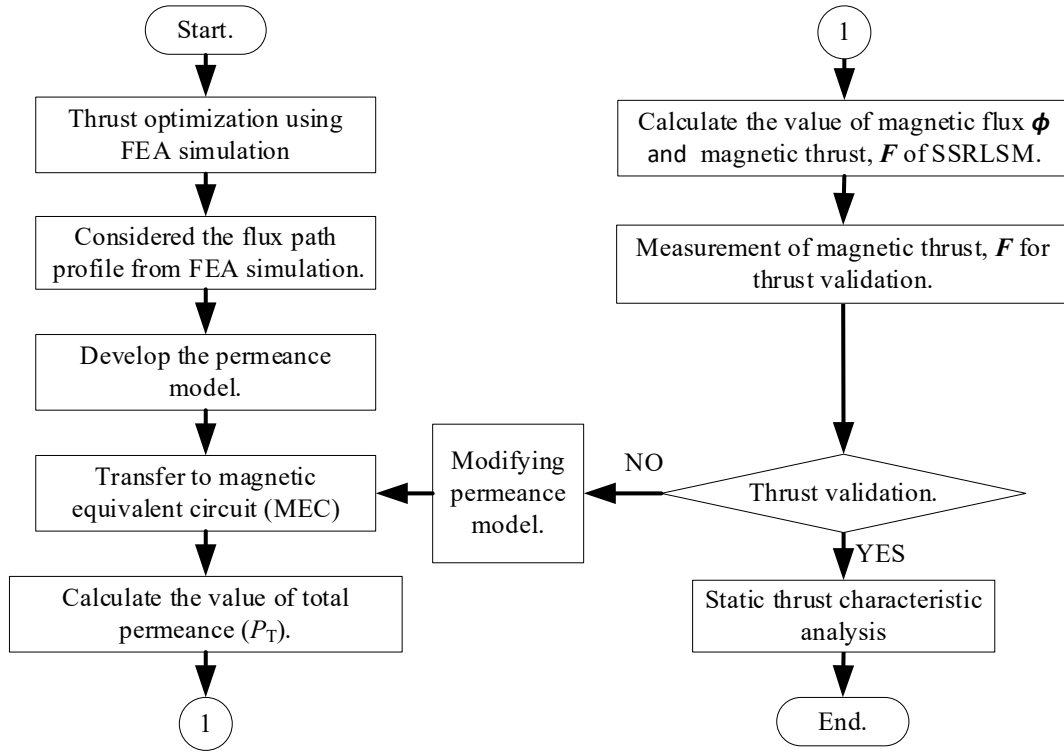


Figure 2. Methodology of the analytical modelling of the SSRLSM using MEC based on PAM.

The permeance model of each position was developed based on the matching flux pattern obtained from the simulation FEM with pole configuration in Table 1, thus the pattern of each permeance was identified. There are nine identified air gap permeances for SSRLSM:  $P_1, P_2, P_3, P_4, P_5, P_6, P_7, P_8$  and  $P_9$ . The combination of these nine permeances will create different permeance models due to different flux patterns as shown in Figure 3. The permeances in the air region are associated with three types of fluxes: the overlap flux between the mover and the stator poles, the overlap flux between the mover and the mover or the overlap flux between the stator and the stator and the fringing flux.

The basic shape of permeance is a rectangular prism and is calculated as Equation (1) [5], [15], [16], [19]. Referring to Equation (1),  $\mu_0$  is the permeability of free space, the value is equal to  $(4\pi \times 10^{-7})$  H/m.  $A$  is the cross-sectional area of the overlapped area between the mover and stator pole for a prism shape and is calculated using Equation (2). The detailed cross-sectional view for one pole of the SSRLSM is presented in Figure 4. The value of the  $w_{m_x}$  refers to the overlapped flux path between the mover and stator and is calculated using Equation (3).  $g$  is the air gap length between the mover and stator poles and  $l_m$  is the stack length of SSRLSM.

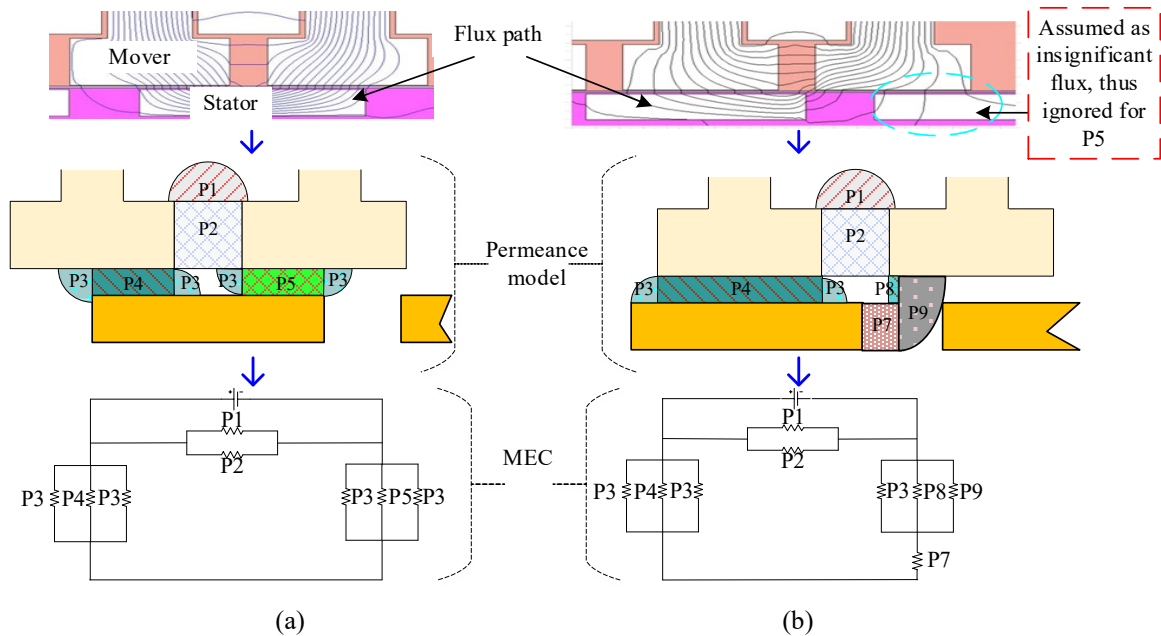
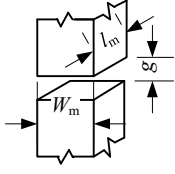
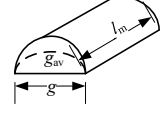
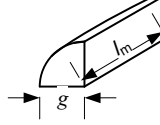
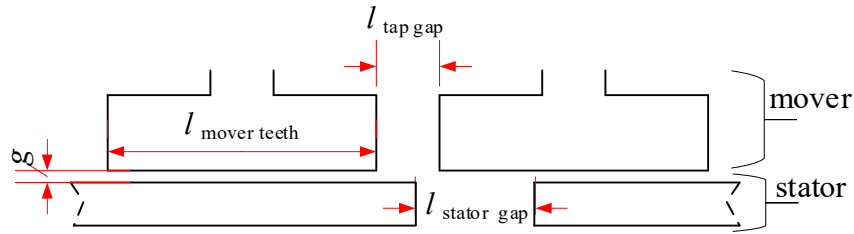


Figure 3. Development of permeance model and MEC for analytical modelling of SSRLSM (a) Fully aligned; (b) Partially aligned.

Table 1. Configuration of poles and air gap.

System	Configuration of poles	Permeance equation	System	Configuration of poles	Permeance equation
1		Rectangular prism: $P_2, P_4, P_5, P_6, P_7, P_8$ $P_x = \frac{\mu_0 A}{g}$ $= \mu_0 \frac{w_m \times l_m}{g}$	2		Half-cylinder: $P_1$ $P_1 = 0.26\mu_0 l_m$
			3		One-quarter of cylinder: $P_3, P_9$ $P_y = P_9$ $= 0.52\mu_0 l_m$

Figure 4. Cross-section outline of  $w_{m_x}$  for overlap poles.

$$P = \frac{\mu_0 A}{g} = \mu_0 \frac{w_{m_x} \times l_m}{g} \quad (1)$$

$$A = (w_{m_x} \times l_m) \quad (2)$$

$$w_{m_x} = l_{mover\ teeth} - (l_{stator\ gap} - l_{tap\ gap}) \quad (3)$$

The permeance for  $P_4, P_5$  and  $P_8$  are the prism pole configuration, thus having the same permeance given in Equation (4). The values of  $P_4, P_5$  and  $P_8$  are different for each position of the mover, depending on the dimension of the  $w_{m_x}$ . Otherwise,  $P_2, P_6$  and  $P_7$  are prism pole configuration but  $w_m$  is constant, and not affected by mover position. The  $w_m$  for  $P_2$  refers to the overlapping flux path between mover poles. While for  $P_6$  and  $P_7$ ,  $w_m$  refers to the overlap flux path between stators poles.

$$P_4 = P_5 = P_8 = \mu_0 \frac{w_{m_x} \times l_m}{g} = (4\pi \times 10^{-7}) \frac{[l_{mover\ teeth} - (l_{stator\ gap} - l_{tap\ gap})] l_m}{0.003} \quad (4)$$

$$P_2 = \mu_0 \frac{w_{m_2} l_m}{g} \quad (5)$$

$$P_6 = \mu_0 \frac{w_{m_6} l_m}{g} \quad (6)$$

$$P_7 = \mu_0 \frac{w_{m_7} l_m}{g} \quad (7)$$

While  $P_1$  is half cylinder and  $P_3$  is half-quarter cylinders, both represent the permeance from the fringing path. The fringing flux path should be regarded as an accurate result. The permeance  $P_9$  has the same shape as  $P_3$  and thus has the same equation. Based on the Equations (8) and (9),  $P_1, P_3$  and  $P_9$  are constant and unaffected by the mover position.

$$P_1 = 0.26\mu_0 l_m \quad (8)$$

$$P_3 = P_9 = 0.52\mu_0 l_m \quad (9)$$

The developed permeance model for aligned and partially aligned positions have different combinations of the individual permeance as shown in Figure 3. This is due to the variation in the magnetic flux produced by the phase windings at different mover positions, thus creating the difference flux pattern for each condition. In the case of the partially aligned position, the

permeance of  $P_5$  was disregarded due to the quantity of the flux flow in stator is insignificant and not concentrated. The developed permeance models are transformed to MEC of SSRLSM as shown in Figure 3. Thus, the formulated expression for total permeance,  $P_T$  is determined from each of the respective MECs of SSRLSM. As a sample, two critical mover positions are given in Equations (10) and (11).

$$P_{T_{Fully\ aligned}} = (P_1 + P_2) // (P_3 + P_4 + P_3) // (P_3 + P_5 + P_3) \quad (10)$$

$$P_{T_{Partially\ aligned}} = (P_1 + P_2) // (P_3 + P_4 + P_3) // (P_3 + P_9 + P_8) // P_7 \quad (11)$$

Referring to the material of the yoke for SSRLSM, based on the  $N$  equal 1800 turns and cross-section area  $A$  for each coil, the magnetic flux density of the SS400 will be saturated at  $2T$ . In the determination of thrust characteristics, the phase current is controlled to avoid the magnetic saturation effect. The flux density  $B_k(i, x)$  in path  $k$  for current  $i$  and position  $x$  is calculated using Equation (12) and related to the magnetic flux  $\phi$ .  $\phi_k(i, x)$  is the magnetic flux and  $A_k$  is the cross-sectional area determined by the geometry of SSRLSM. The magnetic flux is calculated from the permeance as Equation (13). Moreover, the output power of an SSRLSM is calculated using the co-energy, which can be represented as the area between aligned and unaligned flux linkage curves. The magnetic co-energy,  $W$  of the SSRLSM, can be calculated using Equation (14).  $W$  is the magnetic co-energy in Joule and  $N$  is the coil turn. Differentiating the value of magnetic co-energy ( $W$ ) to the mover position will give the value of thrust ( $F$ ) as Equation (15).

$$B_k(i, x) = \frac{\phi(i, x)}{A_k} \quad (12)$$

$$\phi = PNI \quad (13)$$

$$W = N \int_0^I \phi_n dI = NI\phi_n \quad (14)$$

$$F = \frac{\partial W(i, x)}{\partial x} \Big|_{i=\text{const}} = \frac{-\partial W(\phi, x)}{\partial x} \Big|_{\phi=\text{const}} \quad (15)$$

#### 4. COMPARISON OF THE THRUST CHARACTERISTIC

Figure 5(a) shows the characteristics of the magnetic flux density,  $B$  as a function of the mover position. The phase currents considered are 1.2 A, 2 A, 3 A, 4 A and 5 A. When the mover moves from 0 mm to a fully aligned position, the magnetic flux density increases. As the value of the phase current increases, the total magnetic flux in the SSRLSM also increases until it reaches its saturation point, the magnetic flux begins to saturate at  $2T$  when the current reaches 2A. Figure 5(b) illustrates how the magnetic flux  $\phi$  relates to the positions of the mover. When the current exceeds 2 A, the  $\phi$  becomes saturated at 0.16 mWb. The magnetic flux  $\phi$  is proportional to the phase current according to Equation (13). There is no linear relationship between the flux linkage and the current in the saturated region at a fully aligned position.

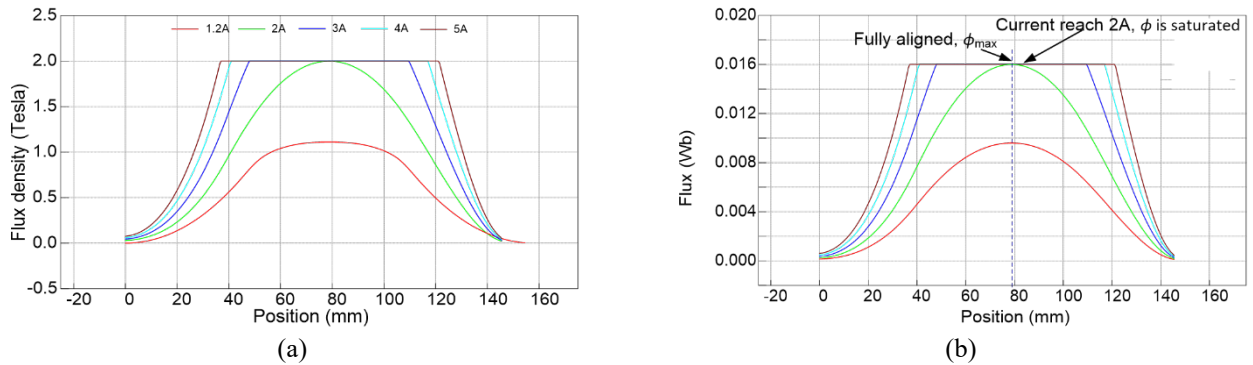


Figure 5. The SSRLSM flux profile for the phase current 1 A - 5 A, (a) Flux density  $B$  against the position of the mover; (b) Flux  $\phi$  against position of mover.

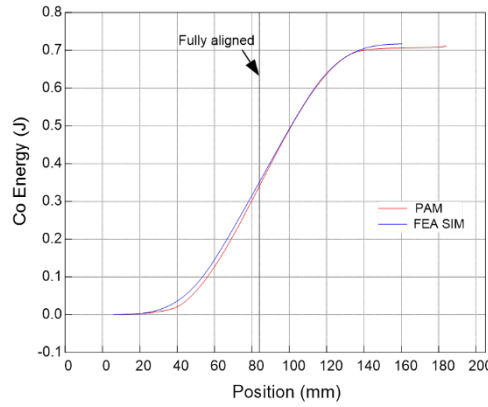
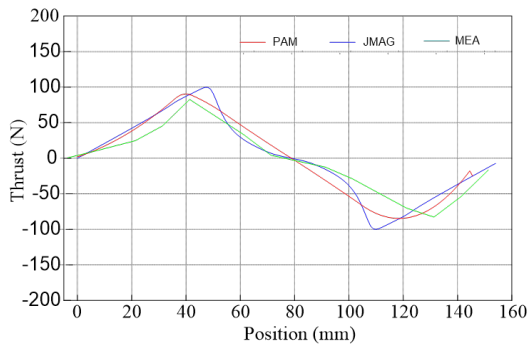
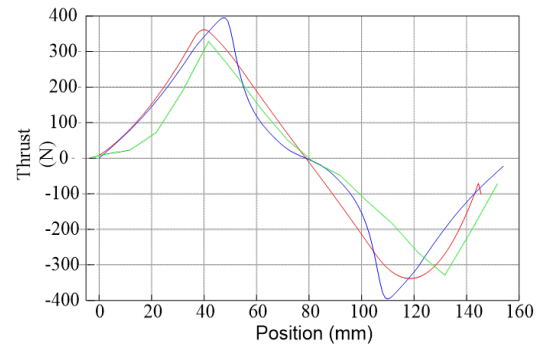


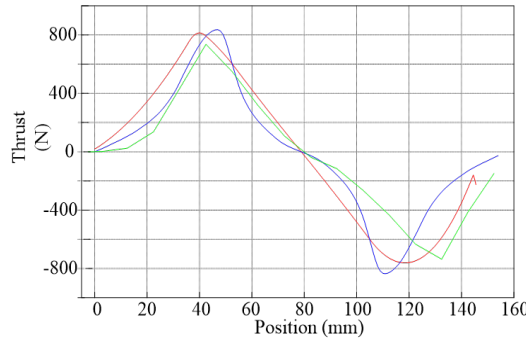
Figure 6 Comparison of magnetic co-energy between PAM and FEM simulation results.



(a)



(b)



(c)

Figure 7. Comparison of thrust characteristic between PAM, FEA simulation and measurement results for phase current, (a) 1 A; (b) 1.2 A; (c) 2 A.

In an SRLSM, the co-energy and the magnetic flux are two essential parameters that are related to each other and play a crucial role in determining the motor's performance in terms of thrust. Figure 6 shows the result of the magnetic co-energy between PAM and the simulation using FEA. The result shows good agreement, thus, to ensure the accuracy and reliability of the developed model. The electromagnetic thrust  $F$  is calculated based on the derivative of the magnetic co-energy  $W$  concerning the mover's position,  $x$ , while keeping the phase current  $i$  constant as Equation (15). The validation of the PAM model is carried out using simulations (FEM) and measurements (MEA), as shown in Figure 7.

To ensure a valid comparison, the thrust results obtained from the PAM and FEM models are scaled down to a quarter of their original values before comparison with the MEA results. This scaling is necessary because the SSRLSM prototype, as shown in Figure 8, was produced on a laboratory scale and is only a quarter of the size of the original model. The prototype was produced on a laboratory scale due to the mechanical issue. The analysis shows that the thrust characteristics of the individual results are in excellent agreement with each other and show only minimal deviations. This result is of great importance as it proves the accuracy and reliability of the proposed approach for modelling the SSRLSM. Consequently, it serves as an alternative and efficient tool for modelling and analysing the performance of electric motors. Moreover, in this study, MEC is considered instead of FEM, where the mathematical equation for the corresponding parameters can be derived from the permeance model. These equations are necessary to obtain information about the interaction between the magnetic flux with the position of the motor and the phase current of the motor. They also help in the development of drivers by enabling fast and accurate calculation of the flux pattern and optimizing motor performance.



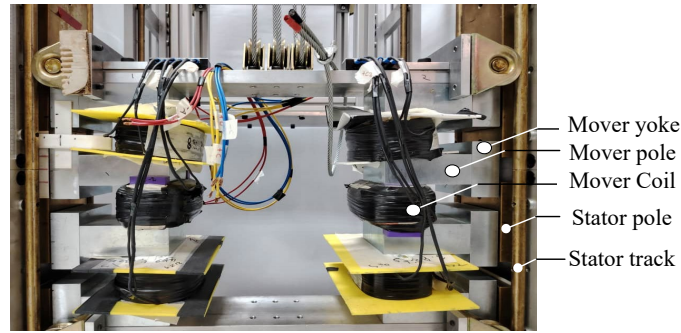


Figure 8. The prototype of the SSRLSM.

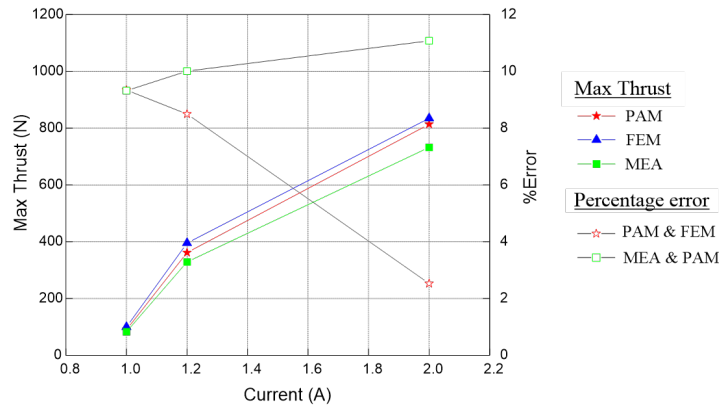


Figure 9. Maximum thrust profile of SSRLSM and percentage error.

Figure 9 shows the comparison of the maximum thrust between PAM, FEM and MEA, and their percentage error. As for the maximum thrust profile, it shows a slight departure occurred between PAM, FEM and MEA due to the accuracy of the modelling of the permeance model as discussed in Section 1. Based on the maximum thrust profile, the percentage error of PAM compared to FEM is calculated, where the percentage error obtained is between 2% to 9%. Otherwise, the percentage error calculated between PAM and MEA is 9% to 11%, it is not far from the acceptable range, between 5%-10% as mention in [15]. The assumption and consideration during the modelling process using PAM are essential, especially considering the fringing flux for achieving an accurate result.

Referring to the previous literature on the validation of the proposed model with simulation FEM and measurement result, comprehensive comparisons between experimental measurements and simulation tools for electromechanical devices is lacking [15]. Apart from a small number of exceptions, the limited number of papers that provide such comparisons claim to have achieved "good agreement," but they demonstrate an error of 10% or more between the test and simulation results [2], [11], [23]–[26]. Many papers that include experimental data failed to compare torque or force results or present any form of error analysis.

## 5. CONCLUSION

Theoretical calculation of the thrust using the MEC method is derived from the developed permeance model of the SSRLSM. The equations obtained were used to study and analyse the characteristics of the thrust performance of SSRLSM. The effect of the mover position and phase current on the thrust has been observed. The derived equation shows that the magnetic flux of SSRLSM exhibits trends with increasing phase current but starts to saturate when the current reaches above 2 A. The trend of magnetic flux over phase current is due to the stator and rotor cores becoming saturated with magnetic flux. Therefore, the magnetic flux density,  $B$  in the cores reaches a level at which the core's permeability can no longer increase, and any additional flux results in no increase in the magnetomotive force (MMF) generated by the mover windings.

The accuracy of the MEC model has been verified through comparisons with FEM and experimental results. The theoretical calculation from PAM is compared to the FEM and MEA values and shows good agreement, although it has a slight deviation. A small deviation can be improved by considering the motor's magnetic path on the developed permeance model. Furthermore, the analytical results are conspicuously influenced by the assumption of the fringing magnetic flux distribution of the air gap. It is essential to build an accurate permeance network and the systematic result taken.

## ACKNOWLEDGEMENT AND FUNDING

The first author thanks Universiti Kuala Lumpur (UniKL) for providing a full-time study leave and to Majlis Amanah Rakyat (MARA) of Malaysia for financial support. Furthermore, all the authors thank the Ministry of Education Malaysia and Universiti Teknikal Malaysia Melaka (UTeM) for providing the FRGS/2018/FKE-CERIA/F00356 research grant.

## DECLARATION OF CONFLICTING INTERESTS

The authors declare no potential conflicts of interest with respect to the research and publication of this article.

## REFERENCES

- [1] D. Wang, Z. Feng and H. Zheng, Comparative analysis of different topologies of linear switched reluctance motor with segmented secondary for vertical actuation systems, *IEEE Transaction on Energy Conversion*, 36(4), 2021, 2634-2645.
- [2] A. Malekpour Shahraky, S. Sheikhanloy, H. Torkaman and M. S. Toulabi, Design and performance prediction of a novel linear switched reluctance motor, *Electric Power Components System*, 49(1-2), 2021, 171-183.
- [3] A. Ghaffarpour, M. Vatani, M. A. J. Kondelaji and M. Mirsalim, Analysis of linear permanent magnet switched reluctance motors with modular and segmental movers, *IET Electric Power Applications*, 17(6), 2023, 756-772.
- [4] N. Abdulah, F. A. A. Shukor, R. N. F. K. R. Othman, S. R. C. Ahmad and N. A. M. Nasir, Modelling methods and structure topology of the switched reluctance synchronous motor type machine: A review, *International Journal of Power Electronics and Drive Systems*, 14(1), 2023, 111-122.
- [5] C. S. Obbu and S. Lakhimsetty, Design of a linear permanent magnet synchronous motor with minimized cogging force, *IEEE IAS Global Conference on Renewable Energy and Hydrogen Technologies (GlobConHT)*, Male, Maldives, 2023.
- [6] D. Wang, X. Du, D. Zhang and X. Wang, Design, optimization, and prototyping of segmental-type linear switched-reluctance motor with a toroidally wound mover for vertical propulsion application, *IEEE Transactions on Industrial Electronics*, 65(2), 2017, 1865-1874.
- [7] R. F. L. Santos and L. A. R. Tria, Evaluation of a modular stator, segmented rotor switched reluctance motor, *IEEE PES Asia-Pacific Power and Energy Engineering Conference (APPEEC)*, Macao, China, 2019, 866-872.
- [8] S. R. Mousavi-Aghdam, M. R. Feyzi and N. Bianchi, Analysis and comparison study of novel stator-segmented switched reluctance motor, *Iranian Journal of Electrical and Electronic Engineering*, 13(1), 2017, 68-76.
- [9] A. Sohrabzadeh, H. Torkaman and A. Yousefi Javid, Improvement undesirable characteristics of the switched reluctance motor with triangular rotor structure, *IEEE Transactions on Energy Conversion*, 38(3), 2023, 2118-2125.
- [10] P. Andrada, B. Blanqué, M. Torrent and P. Kobeaga, Segmented stator switched reluctance motor drive for light electric vehicle, *International Journal of Electrical and Computer Engineering Research*, 3(1), 2023, 18-23.
- [11] CV Aravind, N. Misron, A. Saadha, F. Azhar, A. A. Stonier and D. S. Vanaja, System design, analysis, and experimental investigations of linear switched reluctance machines with double mover configuration, *Journal of Vibration and Control*, 2023.
- [12] F. Rezaee-Alam, A. Nazari Marashi and S. Roozbehani, Modified magnetic equivalent circuit model for magnetic field analysis of one cage-rotor induction motor used in electric submersible pumps, *IET Electric Power Applications*, 17(6), 2023, 802-812.
- [13] W. Uddin and Y. Sozer, Analytical modeling of mutually coupled switched reluctance machines under saturation based on design geometry, *IEEE Transactions on Industry Applications*, 53(5), 2017, 4431-4440.
- [14] G. Davarpanah and J. Faiz, A novel structure of switched reluctance machine with higher mean torque and lower torque ripple, *IEEE Transactions on Energy Conversion*, 35(4), 2020, 1859-1867.
- [15] M. Yilmaz and P. T. Krein, Capabilities of finite element analysis and magnetic equivalent circuits for electrical machine analysis and design, *IEEE Power Electronics Specialists Conference*, Rhodes, Greece, 2008, 4027-4033.
- [16] R. Krishnan, *Switched Reluctance Motor Drives - Modeling, Simulation, Analysis, Design, and Applications*. CRC Press, 2017.
- [17] B. Ganji and M. H. Askari, Analysis and modeling of different topologies for linear switched reluctance motor using finite element method, *Alexandria Engineering Journal*, 55(3), 2016, 2531-2538.
- [18] M. Golzarzadeh and B. Ganji, Analytical modelling of the linear switched reluctance motor with segmental translator, *IET Electric Power Applications*, 13(4), 2019, 527-537.
- [19] M. El-Nemr, M. Afifi, H. Rezk and M. Ibrahim, Finite element based overall optimization of switched reluctance motor using multi-objective genetic algorithm (NSGA-II), *Mathematics*, 9(5), 2021, 576.
- [20] V. Naeini, A detailed magnetic equivalent circuit modeling for torque ripples minimizing of a switched reluctance motor, *International Transactions on Electrical Energy Systems*, 29(10), 2019, 1-14.
- [21] M. Johnson, M. C. Gardner and H. A. Toliyat, A parameterized linear 3D magnetic equivalent circuit for analysis and design of radial flux magnetic gears-Part I: Implementation, *IEEE Transactions on Energy Conversion*, 36(4), 2021, 2894-2902.
- [22] N. A. M. Nasir, F. A. Shukor, N. M. Zuki and R. N. F. K. R. Othman, Design of the segmented-type switched reluctance linear synchronous motor (SSRLSM) for domestic lift application, *Progress In Electromagnetics Research C*, 108, 2021, 13-22.
- [23] G. Davarpanah, S. Mohammadi and J. L. Kirtley, Modelling of switched reluctance machines, *IET Electric Power Applications*, 14(11), 2020, 2146-2153.
- [24] M. A. J. Kondelaji and M. Mirsalim, Segmented-rotor modular switched reluctance motor with high torque and low torque ripple, *IEEE Transactions on Transportation Electrification*, 6(1), 2020, 62-72.
- [25] Y. Hao *et al.*, Torque analytical model of switched reluctance motor considering magnetic saturation, *IET Electric Power Applications*, 14(7), 2020, 1148-1153.
- [26] T. -K. Hoang, L. Vido and D. -Q. Nguyen, A simple approach for air-gap permeance calculations in double excitation synchronous motor modelling with reluctance network, *Vietnam Journal of Science, Technology and Engineering*, 63(2), 2021, 25-31.



